Atomic-resolution study of steps and ridges on arsine-exposed vicinal Ge(100)

W. E. McMahon and J. M. Olson
National Renewable Energy Laboratory, Golden, Colorado 80401
(Received 1 April 1999)

Scanning tunneling microscope images of steps on AsH_3-exposed vicinal Ge(100) show very clearly that As/Ge steps reconstruct. A variety of As/Ge structures based on a ''double-row'' step reconstruction has been observed. We present and discuss some examples, and propose a structural model for a representative two-layer double-row As/Ge step. Under some conditions, we find that atomic-scale ridges are formed at the edges of terraces. These ridges are formed when arsine etching preferentially removes terrace atoms, leaving the steps intact. The resulting ridges are therefore simply the remnants of etch-resistant steps. An atomic-scale model for this process is proposed, and some consequences of ridge formation are discussed. [S0163-1829(99)06727-2]

I. INTRODUCTION

GaAs/Ge is a nearly ideal choice for studies of polar/nonpolar heteroepitaxy. Because GaAs and Ge are lattice matched and have nearly the same coefficients of thermal expansion, it is possible to grow nearly perfect interfaces. In particular, vicinal Ge(100) should provide a good template for GaAs growth. However, even after 30 years of study,[1] there is still no fundamental understanding of the nucleation of GaAs on Ge. Instead, peculiar dependencies associated with growth chamber design and substrate processing history are observed.[2–5]

A survey of the literature reveals two major shortcomings that are largely responsible for this confusion. The first problem is that very little is known about surfaces in a metal-organic chemical-vapor deposition (MOCVD) environment. Despite the fact that most commercial growth of GaAs/Ge is done using MOCVD, most surface characterization studies have been performed for surfaces prepared using molecular-beam epitaxy (MBE). It is not clear how these results can be applied to an MOCVD environment. In our paper, we address this problem directly by using the same ultra-high vacuum (UHV) surface science tools to characterize both MBE- and MOCVD-prepared surfaces. In this paper, we will present results obtained for MOCVD-prepared surfaces.

The second problem is that steps obviously play a crucial role during GaAs nucleation, yet very little is known about their structure (for either MOCVD or MBE). In most cases, the Ge substrate is either intentionally or unintentionally exposed to As prior to GaAs nucleation. It is known that exposure to As can significantly modify the step structure of vicinal Ge,[6,7] suggesting that the atomic structure of As/Ge (arsenic-exposed Ge) steps is different from Ge steps. Nonetheless, an atomic resolution study of As/Ge steps has never been performed.

For this reason, we have conducted an extensive survey of As/Ge steps at atomic resolution with a scanning tunneling microscope (STM). Our data clearly show that As/Ge steps reconstruct, and that at least two different As/Ge step reconstructions exist. In addition, we have found that arsine etching can create atomic-scale ridges at the edges of terraces. This occurs when terrace atoms are preferentially removed, leaving steps intact. This transformation of As/Ge steps into ridges provides some valuable insight into the structure of As/Ge steps.

Although we have observed differences in step structure as a function of arsenic source [AsH_3 (arsine) vs As_4, for example], in this paper we will limit our discussion to AsH_3-exposed Ge.

II. EXPERIMENTAL DETAILS

Commercial Ge(100) substrates miscut 2° or 6° toward (111) or 6° toward (110) were used in this study. Samples were cleaned using a technique similar to that described by Fitzgerald *et al.*[5] They were then loaded into a MOCVD chamber and annealed under 1.2-torr AsH_3 diluted in 70 torr of H_2-carrier gas flowing at 6 standard L/min. Reflectance-difference spectroscopy (RDS) was used to follow surface-phase transitions *in situ*. Stable, nontransient surface phases were quenched to near room temperature under AsH_3, then transferred under vacuum to a UHV analysis chamber for further study. By carefully characterizing all of the various surface phases in this manner, it becomes possible to study and control surface phase transitions in a MOCVD reactor using only RD spectra to identify the various phases.

The analysis chamber is equipped with low-energy electron diffraction, Auger electron spectroscopy (AES), and STM. All surfaces were studied as quenched, with no further treatment after transfer from the growth chamber. Using AES, we checked each sample for surface contamination (carbon, oxygen, or indium, for example). In addition, we are able to record the As and Ge peaks, which in principle can be used to determine the As coverages of our As/Ge surfaces. In practice, we have found that the As/Ge Auger peak intensity ratio (at an incident-beam voltage of 5.0 keV) is nominally 1/15 for most of our As/Ge surfaces. Based on published work,[8] we have assumed that these surfaces are As terminated, with an unknown amount of As diffusion into the Ge substrate. This is consistent with the fact that our As/Ge surfaces are chemically very unreactive, remaining clean under vacuum for many days.

III. DEFINITIONS

To accurately describe a step, at least four parameters must be specified: (1) Step height in layers. 1 layer = 1 Ge

 ©1999 The American Physical Society

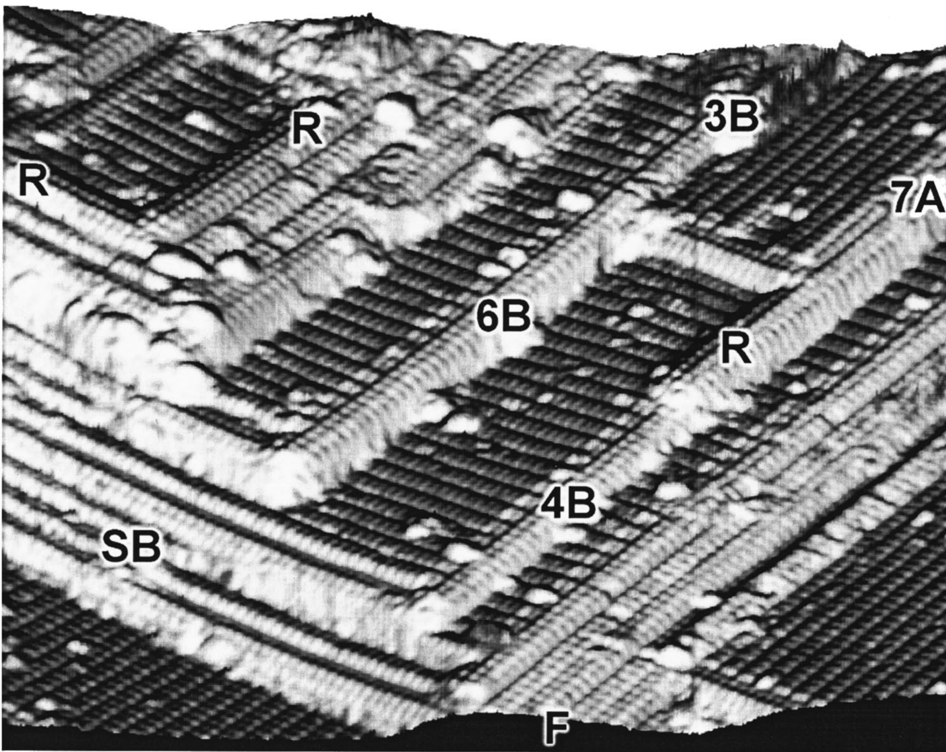

FIG. 1. A 400 Å × 400 Å image of an As/Ge(100) 6°-(110) annealed in a MOCVD chamber under 1.2-torr AsH_3 partial pressure for 20 min at 640 °C. This image has been artificially illuminated from behind the viewer. $V_{sample} = -3.0$ V and $I_{tun} = 0.3$ nA. Some representative DR steps are labeled with their height and type. ''*SB*'' indicates a step-bunched region. ''*F*'' indicates a region where the bunched steps have coalesced into a facet. Ridges are labeled with an ''*R*.''

monolayer (ML) = 1.415 Å = $a_0/4$, where a_0 is the lattice constant of Ge. (2) Step type. For type ''*A*'' (''*B*'') steps, the dimer rows on the upper As/Ge terrace are parallel (perpendicular) to the step edge. For clarity, step height and type may be abbreviated. A ''2-layer type *B*'' step is called a ''2*B*'' step, for example. (3) Step reconstruction. With the exception of 1*A*, 1*B*, and 2*A* steps, we have found that the entire family of As/Ge step reconstructions can be divided into two types. We have chosen to call them ''single-row'' (SR) reconstructions and ''double-row'' (DR) reconstructions. In this paper, we will mainly limit our discussion to DR reconstructions. Because the lack of a DR reconstruction for the 2*A* step is anomalous, a brief discussion of 2*A* steps will also be included at the end of this paper. (4) Surface composition. Steps on clean (As free) Ge are called ''Ge steps,'' whereas steps on arsenic-exposed Ge are called ''As/Ge steps.''

IV. RESULTS

This section will be split into three parts. Part A is an introduction to DR As/Ge steps in which several structural models for a 2*B* DR As/Ge step are considered. Part B is an overview of the As/Ge ridge formation process based upon experimental results. Part C combines the first two parts by testing the various As/Ge step models (Part A) for consistency with the ridge formation process (Part B).

A. Double-row As/Ge steps

Figure 1 serves as an excellent introduction to DR As/Ge steps. In this image one can find a wide variety of different DR structures. It should be noted that we routinely observe the same DR structures for all three of the miscut angles/orientations studied.

The most obvious structures are the type *A* and type *B* DR steps. Despite the (110) miscut of this sample, all steps lie either parallel or perpendicular to the dimer rows. In fact, these step directions are so stable that even small kinks are quite rare. In addition, we have found that AsH_3 exposure can induce step bunching and ''nanofacetting.'' As can be seen in Fig. 1, a facetted region is very well organized compared to a step-bunched region. Not surprisingly, the degree of nanofacetting increases with miscut angle. A more unexpected result is that AsH_3 etching can remove the terrace behind a DR step, creating a ridge. All of this is in sharp contrast to the step morphology of clean Ge, which typically consists of evenly spaced, heavily kinked, single-layer steps lying perpendicular to the miscut direction.[9,10]

1. 2B DR As/Ge steps

A 2*B* DR As/Ge step is shown in Fig. 2. We have chosen this step because it is a particularly clear and simple example. Figure 2(a) shows side and top views of our STM data. The terraces consist of dimer rows, as expected. Each dimer site is labeled with a ''*D*,'' whereas ''*s*1,'' ''*s*2,'' and ''*s*3'' denote step sites imaged by the STM tip as it crossed the step edge. This step topology has been observed with different STM tips on many different samples, ruling out the possibility that this image contains double-tip-generated ''ghost'' sites.

We have chosen to call this a ''double-row'' reconstruction based on the double row of atoms formed by sites *s*1 and *s*2. As mentioned earlier, we have also observed As/Ge steps with only a single row of *s*1 sites. (Single-row steps are not discussed in this paper, however.)

Figures 2(b)-2(f) are ball-and-stick models presented for comparison. These will be referred to as models (b)-(f). A ''*D*'' denotes a dimer atom, whereas numbered sites are la-

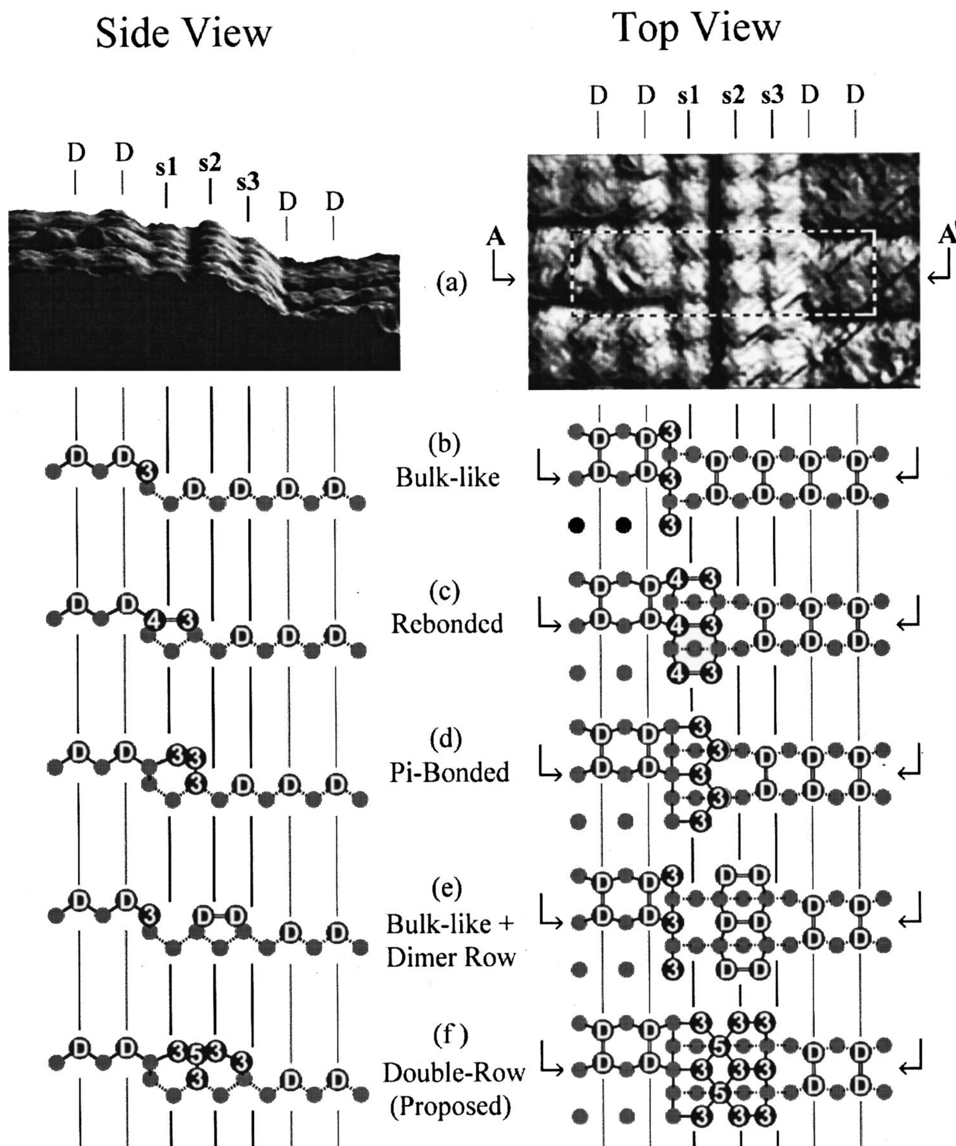

FIG. 2. (a) A high-resolution image of a $2B$ DR As/Ge step. To create this step, a Ge(100) 2°-(111) surface was annealed in a MOCVD chamber at 640 °C for 25 min under 1.2-torr AsH_3 partial pressure. These images have been artificially illuminated from the upper right to reveal the atomic-resolution details. $V_{sample} = -3.0$ V and $I_{tun} = 1.0$ nA. Three step sites are labeled $s1$, $s2$, and $s3$. Dimer sites are labeled D. Models (b)-(f) are aligned below the STM images for ease of comparison. A box in the STM top view defines the area included in each model. The arrows in each top view show the position of line **A**-**A**′.

beled with the number of nearest neighbors. Bulklike or nearly bulklike sites are unlabeled. The lines in our diagrams simply connect nearest-neighbor sites and do not necessarily correspond to chemical bonds. Finally, the chemical identity of individual sites has been left unlabeled.

To first order, we are only interested in the geometry of the various structures, so we considered existing models for Ge, Si, and As/Ge $2B$ steps. Model (b) is a bulklike $2B$ step,[11] model (c) is a rebonded $2B$ step,[12,13] and model (d) is a pi-bonded $2B$ step.[14] None of these three models explains site $s3$, and the bulklike structure cannot explain either site $s2$ or $s3$.

Although these differences are most easily seen in the side views, they are also evident in the top views. For comparison, the line $\mathbf{A}-\mathbf{A}'$ has been indicated with arrows in each top view. In our STM image, three step sites lie along this line. Models (b)-(d) do not support three step sites along this line, and therefore cannot explain the STM topography of this step.

Model (e) is somewhat more promising. It consists of a bulklike $2B$ step plus a single-dimer row.[15] This structure supports three sites along the line $\mathbf{A}-\mathbf{A}'$, but the location of site $s2$ seems to be incorrect. More specifically, in the STM side view, $s2$ and $s3$ do not appear to form the one-dimer-wide terrace predicted by this model.

Because none of the above models seems to fit our data, we propose an alternative [model (f)]. Our proposed model explains the existence and location of all three step sites, assuming that each bright spot in the STM image corresponds to an atom on the surface. Note that this structure can be formed by adding two rows of atoms ($s2$ and $s3$) to a pi-bonded $2B$ step [model (d)]. This alteration converts a threefold site into a fivefold site. Presumably, this fivefold site must be occupied by an As atom, consistent with the fact that DR steps are not formed on clean Ge or Si surfaces.

2. Details

Even if our proposed model is correct, at least two additional details will need to be addressed. The first complication is that it is not known which atoms are Ge and which are As. One possibility is that all of the surface dimers and numbered atoms in our ball-and-stick diagrams are As, whereas the other (bulklike) atoms are Ge. In this case, each bright

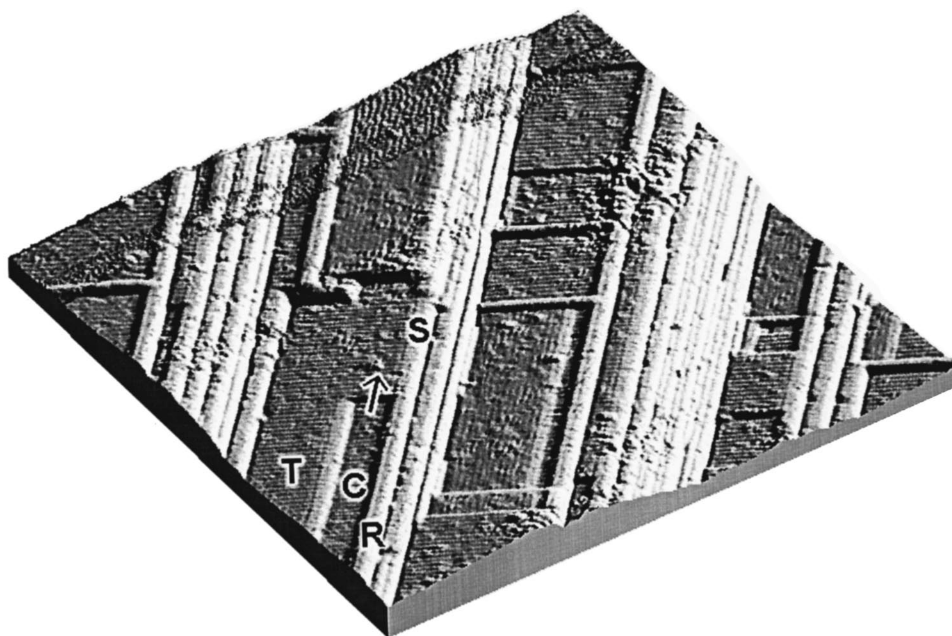

FIG. 3. A $1000\,\text{Å} \times 1000\,\text{Å}$ image of As/Ge(100) 6°-(111) annealed in a MOCVD chamber under 1.2-torr AsH_3 partial pressure for 30 min at 640 °C, then for an additional 15 min at 520 °C. $V_{sample} = -3.0$ V and $I_{tun} = 0.3$ nA. This image has been artificially illuminated from the right. Crater *C* is two layers below terrace *T*. As AsH_3 etches terrace *T* in the direction of the arrow, step *S* is transformed into ridge *R*.

spot in our STM image would correspond to the lone electron pair of a surface As atom.

The second complication is that the presence of hydrogen on these surfaces could induce a myriad of structural permutations. Unfortunately, Auger electron spectroscopy is not sensitive to hydrogen, so we do not know if it is present on the surface.

B. As/Ge ridge formation

In this section, we will show how AsH_3 etching can transform a DR As/Ge step into a ridge. Atomic-scale structural models for this process will be presented in Part C.

1. Arsine etching

Macroscopically, we have found that AsH_3 etches Ge surfaces. Etch rates were determined by measuring height differences between masked and unmasked portions of samples after etching under AsH_3. The etch rate varies slowly with temperature and is approximately linear with AsH_3 partial pressure, with a value of 2000 Å/h at 660 °C under 1.2-torr AsH_3 for a Ge(100) 6°-(110) substrate. A more thorough study of the etch rate as a function of substrate misorientation angles and directions may provide useful information about the etching process.

2. Ridge formation

Microscopically, this etching can occur in a rather unexpected way. STM images show that under some conditions, the terrace *behind* a DR As/Ge step can be etched away, transforming the step into a ridge. In other words, DR steps are more resistant to AsH_3 etching than terraces. The resulting As/Ge ridges are not rare; they have been observed on samples with a variety of miscuts and processing histories.

Since we have only observed ridge formation from DR As/Ge steps, the modifiers ''DR'' and ''As/Ge'' are superfluous. For the remainder of this paper, ''step'' will mean ''DR As/Ge step,'' and ''ridge'' will mean ''As/Ge ridge.''

Figure 3 shows ridge formation on a (111)-miscut surface. This surface was etched under 1.2-torr AsH_3 partial pressure for 30 min at 640 °C, then for an additional 15 min at 520 °C. We have chosen this image because it contains a particularly clear example of the ridge formation process. Consider the effect of AsH_3 etching on crater *C*, which is two monolayers lower than terrace *T*. As etching enlarges crater *C* in the direction of the arrow, step *S* is converted into ridge *R*. Many other examples of ridges in various stages of formation can be found in this image.

3. Atomic-scale etching

Figure 4 provides a more detailed view of ridge formation on a (110)-miscut surface. In this image, etching of terraces $T0$ and $T1$ is exposing terrace $T2$. If additional atoms are removed from terrace $T1$, terrace $T2$ will expand to the left, lengthening ridge $R1$ at the expense of step $S1$. Similarly, if atoms are removed from terrace $T0$, terrace $T2$ will expand toward the back of the image, and ridge $R2$ will grow at the expense of step $S2$.

Steps $S1$ and $S2$ are basically taller versions of the step shown in Fig. 2. Although the steps in Figs. 2 and 4 are different heights, the tops of the steps appear to be identical. In fact, sites $s1$, $s2$, and $s3$ seem to be the same for all DR steps, independent of step height. Furthermore, these sites remain intact during the ridge formation process, so ridges must be structurally similar to DR steps.

Figure 5 shows schematically how AsH_3 etching can form the structures shown in Fig. 4. Figure 5(a) shows the original terrace before etching, with steps leading downhill from two sides. Only the top portion of each step is shown. The step bases have been omitted for clarity. Figure 5(b) shows the same area after the partial removal of terrace $T0$. In Fig. 5(c), terrace $T1$ has also been partially removed. Figure 5(d) is a top view of Fig. 4.

Using these diagrams, the transformation of a step into a ridge can be followed. First consider the type ''*A*'' step in Fig. 5(a). Removal of one layer of terrace atoms converts it into a type ''*B*'' step [Fig. 5(b)]. Removal of a second layer

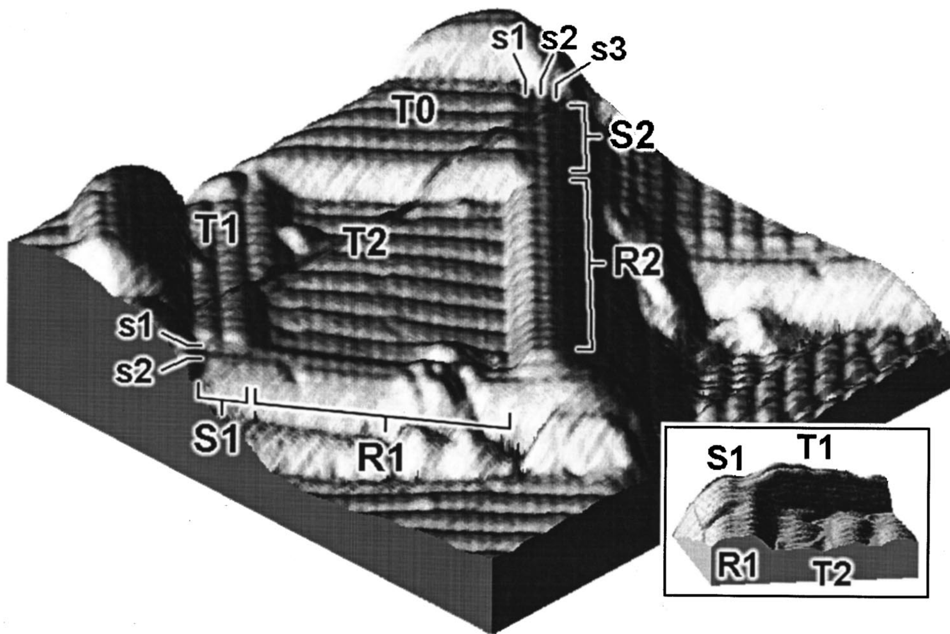

FIG. 4. A 200 Å × 200 Å image of As/Ge(100) 6°-(110) annealed in a MOCVD chamber under 1.2-torr AsH_3 partial pressure for 20 min at 640 °C. $V_{sample} = -3.0$ V and $I_{tun} = 0.3$ nA. This image has been artificially illuminated from the left. AsH_3 etching of this terrace is converting steps $S1$ and $S2$ into ridges $R1$ and $R2$. Ridge $R1$ is more clearly seen in the side view (inset).

of terrace atoms converts part of this type ''B'' step into a $1A$ ridge [Fig. 5(c)]. The ''1'' indicates that the ridge is one-layer tall, while the ''A'' indicates the dimer row direction of the terrace behind the ridge. Notice the appearance of site $s0$ between the $1A$ ridge and terrace $T2$ in Fig. 5(c).

Now consider the evolution of the type ''B'' step in Fig. 5(a). Removal of one layer of terrace atoms converts it into a $1A$ ridge [Fig. 5(b)]. Removal of a second layer of terrace atoms converts it into a $2B$ ridge [Fig. 5(c)]. Once again, the ''2'' indicates the ridge height in layers, while the ''B'' indicates the dimer-row direction on the terrace behind the ridge. Notice the appearance of site $s0$ in Fig. 5(b).

Figure 5(c) can now be compared directly to our data [Fig. 5(d)]. In particular, note that $R1$ is a $1A$ ridge, whereas

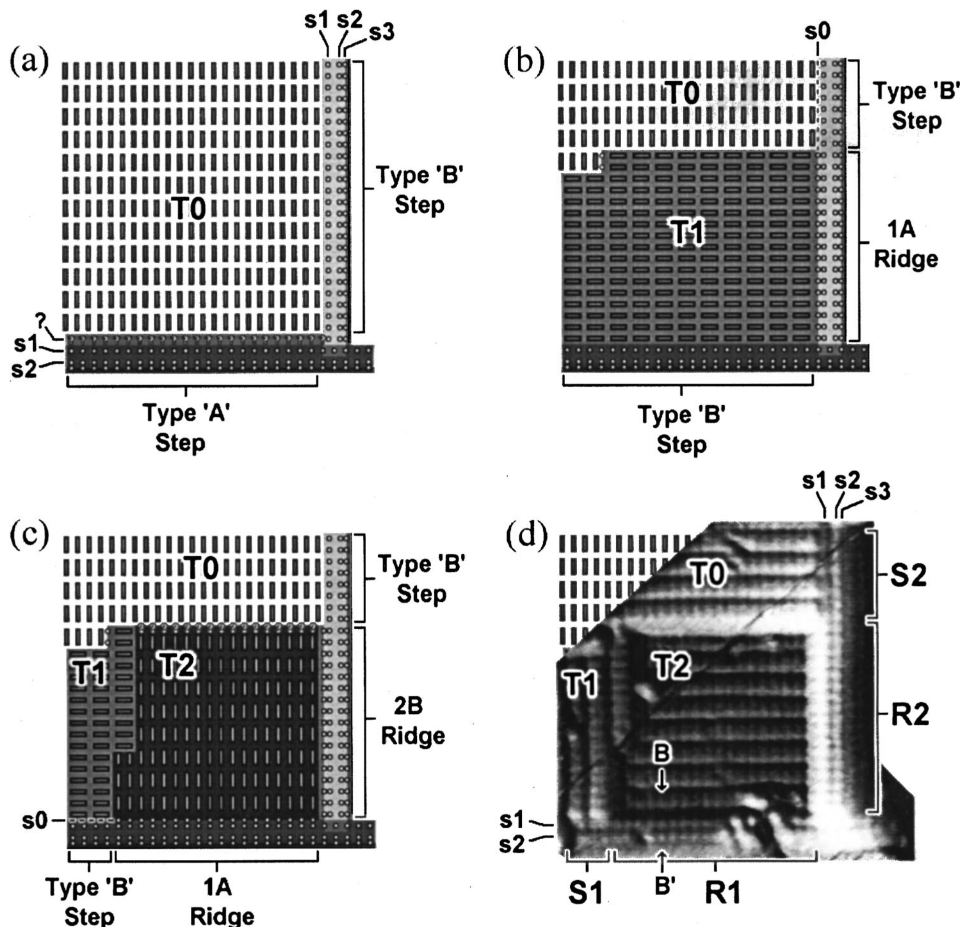

FIG. 5. Schematic diagrams showing how etching can convert steps into ridges. In these diagrams, the shading indicates height. The darker areas are lower than the lighter areas. (a) Terrace $T0$ before etching. Steps lead downhill from two edges of the terrace. (b) Part of terrace $T0$ has been removed, revealing terrace $T1$. (c) Part of terrace $T1$ has been removed, revealing terrace $T2$. (d) A top view of Fig. 4, included for comparison. This top view has been artificially illuminated from the lower left. In (a) and (c), question marks (''?'') indicate sites where the exact structure is not known.

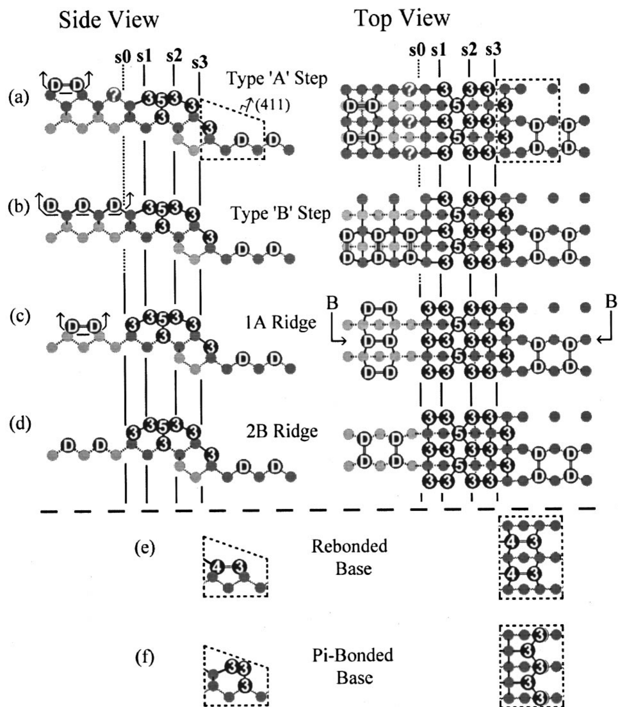

FIG. 6. (a)-(d) Ball-and-stick diagrams for the ridge formation process, based upon our proposed DR As/Ge step model [Fig. 2(f)]. Each structure is created by removing one layer of terrace atoms from the structure above it on the page (as indicated by arrows in the side views). Line **B**-**B**′ is included as a guide for comparison with the data in Fig. 5(d). Alternative step bases are shown in (e) and (f).

$R2$ is a $2B$ ridge. For a $1A$ ridge, sites $s1$ and $s2$ are aligned with terrace dimers [line **B**-**B**′ in Fig. 5(d)]. The apparent heights of ridges $R1$ and $R2$ above terrace $T2$ are 0.5 and 1.5 ML (± 0.2 ML), respectively. Attempts to determine these heights more accurately are hindered both by imperfections and distortions intrinsic to STM, and by variations in apparent height due to electron charge transfer laterally along the sample surface.

C. Atomic-scale models for ridge formation

Using ball-and-stick models, it should be possible to explain how ridge formation occurs at an atomic level. In Figs. 6, 7, and 8, we attempt to explain ridge formation using three of the models presented in Part A (Fig. 2). We will begin with a thorough discussion of our proposed model (Fig. 6), then briefly discuss two counter examples (Figs. 7 and 8).

1. Proposed model

Our proposed model for the ridge formation process is shown in Fig. 6. Figure 6(a) is a $5A$ step based upon our proposed DR structure [Fig. 2(f)]. Although this choice of step height is somewhat arbitrary, only steps with a height of three layers or more can be converted into ridges. For this reason, a two-layer step base (enclosed in a dashed box) has been added. The details of the step base will be discussed shortly and can be ignored for now.

Figures 6(b)–6(d) are created by sequentially removing layers of upper-terrace atoms, as indicated by the arrows in the side views. The resulting sequence of structures can be compared to the corresponding structures in Figs. 4 and 5. Notice that in this model, the positions of sites $s1$, $s2$, and $s3$ remain unchanged during the ridge formation process. Also, upon the formation of a $1A$ ridge, site $s0$ appears, creating a ridge that is symmetric about a plane between $s1$ and $s2$. The same symmetry is apparent in our STM images.

As a final consistency check between our model and the data, compare the top view of Fig. 6(c) with ridge $R1$ in Fig. 5(d). Notice that in both the data and our model, a line drawn through the upper-terrace dimers passes through sites $s1$ and $s2$. [The position of this line is indicated by **B**-**B**′ in both Figs. 5(d) and 6(c).]

As a final detail, it is important to consider the structure of the step base. For the purposes of illustration, we have arbitrarily drawn a bulklike (111)-terminated step base. However, there is no direct experimental evidence for this choice. In fact, we find that bunched steps and nanofacets tend toward an ($n11$) termination, where n is between 3 and 5, not 1. This suggests that a (111)-terminated step base is unlikely, and alternative step bases tending toward a (411) termination must be considered.

To construct a (411)-terminated step base, one must fill the dashed box indicated in Fig. 6(a). Two possible structures are shown in Figs. 6(e) and (f). Although these two structures are simple and familiar, a theoretical comparison of just these two structures would be inconclusive. STM images of Ge and As/Ge ($n11$) surfaces suggest that additional structures should also be considered. Within the context of As/Ge ridge formation this point may merely be academic, but within the context of GaAs/Ge film nucleation, the exact structure of the step bases may be critical. The ridge formation process offers a somewhat unique opportunity for testing theoretical models of step bases.

For type ''A'' steps there is another minor complication. In Fig. 6(a), we have labeled one site with a ''?''. This site corresponds to the ''?'' sites in Fig. 5(a). The structure in this region of type ''A'' steps is unknown. Unfortunately, STM images of this portion of the structure are difficult to interpret.

2. Counter-examples

Figures 7 and 8 are counter examples. Each of these two figures is based upon an alternative model for DR steps. Our

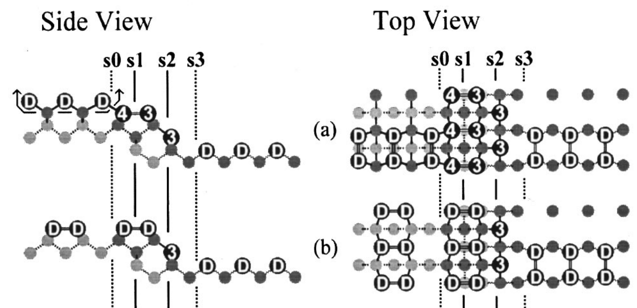

FIG. 7. (a) A $4B$ rebonded step [based upon Fig. 2(c)]. Although this model is inconsistent with our images of $2B$ DR steps, it nonetheless serves as a useful counter-example. (b) Removing one layer of terrace atoms creates a $3A$ bulklike step. This model cannot explain the existence of $1A$ ridges.

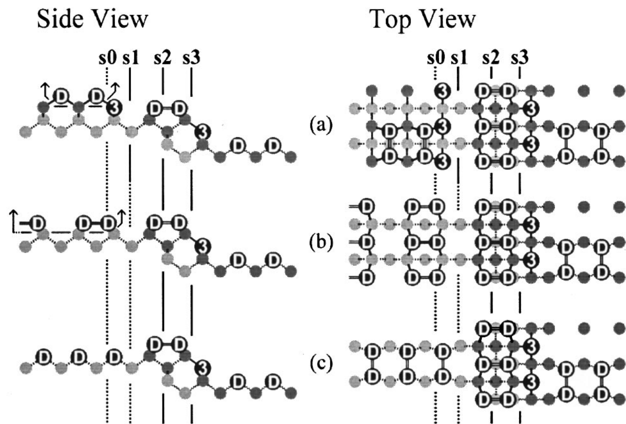

FIG. 8. (a) A bulklike $4B$ step with an intermediate one-dimer-wide terrace [based upon Fig. 2(e)]. (b) Removing one layer of terrace atoms creates a $3A$ step. Although it is within the realm of possibility that this structure explains $2B$ DR steps, it fails to explain the existence of $1A$ ridges. (c) If another layer of terrace atoms is removed, the resulting ridge would be formed by $s2$ and $s3$, *not* $s1$ and $s2$, as seen in our STM images.

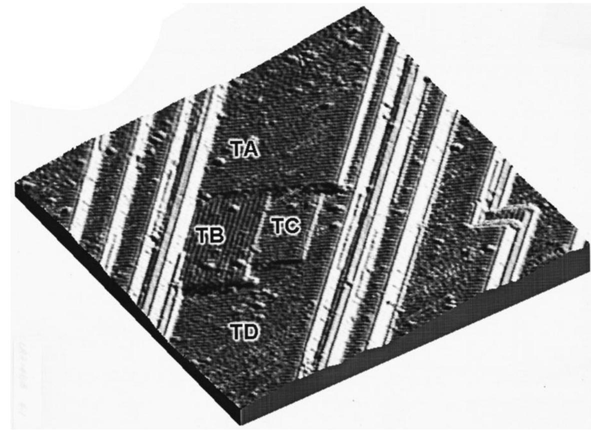

FIG. 9. A 700 Å×700 Å image of As/Ge(100) 6°-(111) annealed in a MOCVD chamber at 650 °C for 15 min under 1.2-torr AsH_3 partial pressure, then for an additional 15 min under 0.24-torr AsH_3 partial pressure. $V_{sample} = +2.0$ V and $I_{tun} = 1.0$ nA. This image has been artificially illuminated from the right. Under these conditions, terraces *TA*, *TB*, and *TC* are being sequentially etched to expose terrace *TD without* forming ridges.

discussion of $2B$ DR steps showed that these models do not seem to be correct. Here, we will show how that ridge formation process can be used as a much more effective test. Notice Figs. 7 and 8 do not begin with a $5A$ step (as did Fig. 6). Instead, they begin with a $4B$ step [equivalent to Fig. 6(b)]. These counter examples are not sensitive to the structure of the bases, so we have chosen the simplest, (111)-terminated step bases for the purposes of illustration.

Our first counter example is a $4B$ rebonded step [Fig. 7(a)]. It is simply a taller version of a rebonded $2B$ step [Fig. 2(c)]. Figure 7(b) shows the same structure with one layer of terrace atoms removed. The result is a bulklike $3A$ step. In other words, this model does not explain the existence of a $1A$ ridge. On this basis alone it is possible to conclude that DR steps cannot be based upon the rebonded structure shown in Fig. 7(a).

A second counter example is based upon the $2B$ step shown in Fig. 2(e). It consists of a bulklike $4B$ step with an intermediate one-dimer-wide terrace [Fig. 8(a)]. In Fig. 8(b), one layer of terrace atoms has been removed. The result is the same as Fig. 7(b)—a $3A$ step with no ridge. If an additional layer of terrace atoms is removed, it is possible to form a ridge out of the row of dimers. Aside from the implausibility of this structure, the resulting ridge is formed form sites $s2$ and $s3$ (not $s1$ and $s2$, as is seen in our data). Once again, we are able to conclude that the structure shown in Fig. 8(a) is not a reasonable DR step structure.

Although counter-examples based upon bulklike [Fig. 2(b)] and pi-bonded [Fig. 2(d)] steps could also be provided, our point is simply to show that ridge formation provides an excellent test for determining whether or not a DR step model is reasonable. Although the above discussion does not prove that our model for a DR step is correct, we have shown that it is consistent with our observations of ridge formation. This is an important criterion that must also be met by alternative DR step models.

3. Details

Even if our proposed model for the etching process is correct, there are some additional complications that must be addressed. As with our models for a $2B$ As/Ge step, it is not known which atoms are As and which are Ge. In addition, the presence and location of hydrogen is unknown.

A final complication is that the etching process must involve more than a simple removal of atoms. To simply remove surface atoms would result in a clean Ge surface, so part of the etching process must involve replacing some Ge atoms with As atoms.

V. DISCUSSION

A. Ridge formation

Regardless of their exact structure, the existence of As/Ge ridges has some important consequences. The first is that As/Ge ridges might affect GaAs nucleation. It is, therefore, important to be aware of their existence, and to understand what factors lead to their formation and destruction. As an example, we reannealed the sample shown in Fig. 3 under a reduced AsH_3 partial pressure at a higher temperature. Afterwards, no ridges were observed with STM. Another example of a ridge-free As/Ge surface is shown in Fig. 9. Terraces *TA, TB*, and *TC* are being sequentially etched to expose terrace *TD*, yet no ridges are observed.

One explanation is that there is some threshold temperature above which the etch rate of steps/ridges rises dramatically to match that of the terraces. Another explanation is that at higher temperatures, surface annealing destroys ridges as fast as AsH_3 etching creates them. Most likely, the truth is a combination of these two explanations. A study of ridge formation as a function of AsH_3 partial pressure and temperature might provide some answers.

The second effect of ridges on As/Ge surfaces concerns step bunching. Aside from any energy-minimization considerations, the bunching of steps can be affected by the kinetics of the etching process. Specifically, the resistance of the DR structure to AsH_3 etching allows it to temporarily protect any steps that have accumulated beneath it. This effect is only temporary, though. Notice that in Fig. 3 most craters are bounded by one- and two-layer ridges, even though hundreds

of layers of Ge have been removed. This implies that ridges taller than two layers are easily destroyed.

A more subtle point is that for the conditions we have studied, two-layer steps do not form ridges. This explains why all ridges are found sitting on top of steps, as opposed to being in the middle of terraces. For example, in Fig. 3 the two-layer steps bounding crater *C* are not forming ridges. Step *S* is able to form a ridge because it is taller than two layers. It is possible that strain near taller steps serves to anchor the ridges. It is also possible that the stability of the upper portion of a step depends upon the structure of its base. Although the exact reason is not known, the result is a surface that remains relatively smooth during the AsH_3-etching process. If two-layer steps formed ridges, AsH_3 etching could form ridges anywhere on a terrace, quickly covering the entire surface with ridges.

B. 2*A* As/Ge steps

As a final note, it is important to discuss the lack of a DR (or SR) reconstruction for 2*A* As/Ge steps. Although they might reconstruct in some subtle way, 2*A* As/Ge steps appear to be nominally bulklike in our STM images. The step between terraces *T*0 and *T*2 in Figs. 4 and 5(d) is an excellent example.

The lack of a 2*A* SR or DR reconstruction may prove to be an excellent test for theoretical models of DR reconstructions. In other words, any theory that explains DR reconstructions must also explain why 2*A* steps are not DR reconstructed. It is also interesting to note that 2*A* As/Ge steps are somewhat rare, suggesting that they are high-energy steps that only form as a result of topological constraints imposed by neighboring steps and terraces. The only other unreconstructed As/Ge steps are 1*A* and 1*B* steps, but this is not surprising because single-layer steps are not tall enough to support a DR reconstruction.

VI. CONCLUSIONS

In conclusion, we have conducted an extensive STM study of arsenic-exposed vicinal Ge(100) surfaces and found that most As/Ge steps are reconstructed. We have observed two types of step reconstructions, which we have chosen to call ''single-row'' (SR) and ''double-row'' (DR) reconstructions. Three exceptions are 1*A*, 1*B*, and 2*A* steps, which do not support SR or DR reconstructions. In this paper, we presented examples of double-row structures resulting from AsH_3 exposure, and proposed a structural model for a representative DR step.

In addition, we have observed that AsH_3 etches Ge surfaces. Under some conditions, AsH_3 etching can convert steps into ridges. In other words, steps are more resistant to AsH_3 etching than terraces.

Using ball-and-stick models, we have shown that our proposed model for double-row As/Ge steps is consistent with the ridge formation process. Counter examples are provided showing how two alternative structures are not consistent with our observations of ridge formation. Ridge formation can, therefore, be used to test the plausibility of proposed DR step models. We have also shown that by changing the temperature and AsH_3 partial pressure, it is possible to AsH_3-etch Ge surfaces *without* forming ridges.

At the very least, the existence or absence of atomic-scale ridges adds an interesting characteristic to the surface phase diagram of As/Ge. At a more fundamental level, the As/Ge ridge formation process provides an interesting opportunity for testing theoretical models of surface structures and processes.

ACKNOWLEDGMENTS

This work would not have been possible without the help of J. Geisz, A. Kibbler, D. Friedman, S. Kurtz, C. Kramer, and K. Jones. In addition, we would like to thank B. Nosho, S. Ringel, E. Fitzgerald, S. Ting, R. Hicks, and H. Farrell for their helpful discussions. This work was supported by the Office of Energy Research, Basic Energy Sciences, U.S. Department of Energy under Contract No. DE-AC 36-98-GO 10337.

[1] L. C. Bobb, H. Holloway, and K. H. Maxwell, J. Appl. Phys. **37**, 4687 (1966).

[2] J. C. Chen, M. L. Ristow, J. I. Cubbage, and J. G. Werthen, J. Electron. Mater. **21**, 347 (1992).

[3] Y. Li, G. Salviati, M. M. G. Bongers, L. Lazzarini, L. Nasi, and L. J. Giling, J. Cryst. Growth **163**, 195 (1996).

[4] C. Pelosi, G. Attolini, C. Bocchi, P. Franzosi, C. Frigeri, M. Berti, A. V. Drigo, and F. Romanato, J. Electron. Mater. **24**, 1723 (1995).

[5] E. A. Fitzgerald, J. M. Kuo, Y. H. Xie, and P. J. Silverman, Appl. Phys. Lett. **64**, 733 (1994).

[6] P. R. Pukite and P. I. Cohen, J. Cryst. Growth **81**, 214 (1987).

[7] S. Gan, L. Li, M. J. Begarney, D. Law, B.-K. Han, and R. F. Hicks, J. Appl. Phys. **85**, 2004 (1999).

[8] J. F. Morar, U. O. Karlsson, R. I. G. Uhrberg, J. Kanski, P. O. Nilsson, and H. Qu, Surf. Sci. **41/42**, 312 (1989).

[9] J. E. Griffith, J. A. Kubby, P. E. Wierenga, R. S. Becker, and J. S. Vickers, J. Vac. Sci. Technol. A **6**, 493 (1988).

[10] B. Röttger, T. Bertrams, and H. Neddermeyer, J. Vac. Sci. Technol. B **14**, 925 (1996).

[11] O. L. Alerhand, J. Wang, J. D. Joannopoulos, and E. Kaxiras, J. Vac. Sci. Technol. B **9**, 2423 (1991).

[12] D. J. Chadi, Phys. Rev. Lett. **59**, 1691 (1987).

[13] T. Komura, M. Yoshimura, and T. Yao, J. Vac. Sci. Technol. B **14**, 906 (1996).

[14] D. E. Aspnes and J. Ihm, Phys. Rev. Lett. **57**, 3054 (1986).

[15] H. Itoh, S. Narui, Z. Zhang, and T. Ichonokawa, Surf. Sci. Lett. **277**, L70 (1992). (The structure we show is actually a variation of the structures presented in this reference.)